JACS
JOURNAL OF THE AMERICAN CHEMICAL SOCIETY
Article
Cite This: J. Am. Chem. Soc. 2018, 140, 827−833
pubs.acs.org/JACS

Universal Relationship between Molecular Structure and Crystal Structure in Peptoid Polymers and Prevalence of the *cis* Backbone Conformation

Douglas R. Greer,[†,‡] Michael A. Stolberg,[†] Joyjit Kundu,[§,⊥] Ryan K. Spencer,[∥] Tod Pascal,[§] David Prendergast,[§] Nitash P. Balsara,[*,†,‡] and Ronald N. Zuckermann[*,§]

[†]Materials Sciences Division, Lawrence Berkeley National Laboratory, Berkeley, California 94720, United States
[‡]College of Chemistry, University of California, Berkeley, Berkeley, California 94720, United States
[§]Molecular Foundry, Lawrence Berkeley National Laboratory, Berkeley, California 94720, United States
[∥]Department of Chemistry and Department of Chemical Engineering & Materials Science, University of California, Irvine, Irvine, California 92697, United States

Supporting Information

ABSTRACT: Peptoid polymers are often crystalline in the solid-state as examined by X-ray scattering, but thus far, there has been no attempt to identify a common structural motif among them. In order to probe the relationship between molecular structure and crystal structure, we synthesized and analyzed a series of crystalline peptoid copolymers, systematically varying peptoid side-chain length (S) and main-chain length (N). We also examined X-ray scattering data from 18 previously reported peptoid polymers. In all peptoids, we found that the unit cell dimensions, a, b, and c, are simple functions of S and N: a (Å) = 4.55, b (Å) = [2.98]N + 0.35, and c (Å) = [1.86]S + 5.5. These relationships, which apply to both bulk crystals and self-assembled nanosheets in water, indicate that the molecules adopt extended, planar conformations. Furthermore, we performed molecular dynamics simulations (MD) of peptoid polymer lattices, which indicate that all backbone amides adopt the *cis* conformation. This is a surprising conclusion, because previous studies on isolated molecules indicated an energetic preference for the *trans* conformer. This study demonstrates that when packed into supramolecular lattices or crystals, peptoid polymers prefer to adopt a regular, extended, all-*cis* secondary structure.

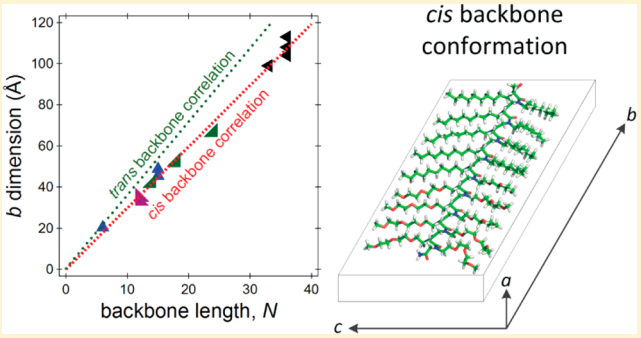

INTRODUCTION

Poly N-substituted glycine materials (peptoids) have the capacity for prolific diversity due to a large library of monomers, synthetic sequence control, and monodispersity.[1−4] These properties make peptoids an ideal platform with which to study the relationship between chemical structure and folded or supramolecular structure.[5,6] Additionally, peptoids are nontoxic and can self-assemble in water, providing a useful platform for biomimetic, foldamer, and nanoscale research.[7,8] Though peptoids are generally thought to be flexible in solution,[9,10] many well-defined molecular structures have been identified, typically from short oligomers. Ribbons,[11] loops,[12] helices,[13,14] and macrocycles[15,16] have been observed in short chains, all resulting from the deliberate introduction of conformational constraints (e.g., sterically hindered monomers). Higher molecular weight peptoid polymers (> 10mers) are receiving increased attention,[2,3] due to their convenient and efficient synthesis,[17] and a growing interest in the impact of sequence-control on polymer properties.[18] Peptoid polymer structure in the bulk phase has been probed by many investigators, but so far, there has been no consensus on identifying any underlying common motifs to their structure or packing interactions.

The unit cell dimensions of several crystalline peptoid polymers in the bulk state (i.e., without solvent) have been previously reported. Rosales et al.[19] and Lee et al.[20] have studied the effect of side-chain length on unit cell dimensions in peptoid homopolymers, and Sun et al.[21,22] have studied the crystal structure of diblock copolypeptoids. Peptoid diblocks with appropriate hydrophobic and hydrophilic domains have also been shown to form crystalline nanosheets in aqueous solution.[23] These sheets have lengths and widths of at least hundreds of nanometers and have thicknesses on the order of a few nanometers, and are a useful platform for mimicking cell membranes.[24] Thus, far, there has been no complete attempt to relate the crystal structure observed in these studies[19−23,25] to molecular structure. In particular, all of these studies present

Received: November 8, 2017
Published: January 8, 2018

DOI: 10.1021/jacs.7b11891
J. Am. Chem. Soc. 2018, 140, 827−833

the peptoid backbones in the *trans* conformation without clear evidence.

In order to systematically probe the relationship between molecular structure and crystal structure, we synthesized a series of peptoid block copolymers to explore the dependence of unit cell dimensions on side-chain length (S) and backbone main-chain length (N). We use small angle and wide-angle X-ray scattering (SAXS and WAXS) to examine the lattice dimensions, and molecular dynamics simulations on a representative peptoid polymer to interpret the data at the molecular level. Unexpectedly, we discovered a unifying relationship between molecular structure and crystal structure using S and N as the sole parameters. This relationship, which applies to all of the known peptoid polymer crystals reported in the literature,[19−23,25] indicates the prevalence of the *cis* backbone conformation in both peptoid bulk phases and in certain supramolecular assemblies.

RESULTS AND DISCUSSION

Peptoid polymers are thought to pack into extended conformations in the bulk phase,[20,21] and their backbone configuration and is most often depicted in a *trans* conformation (Figure 1). We designed a set of acetylated

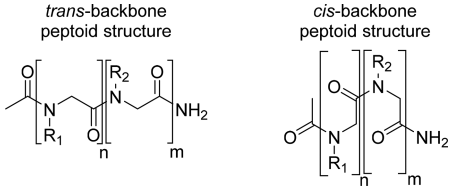

Figure 1. Extended peptoid diblock copolymers, shown in an all *trans* (left) and an all *cis* (right) configuration, with side chains R_1 and R_2. The main-chain length (N) listed in Table 1 is equal to $n + m$.

peptoid polymers based on a diblock family consisting of one crystalline, hydrophobic block based on *n*-alkane side chains, and a noncrystalline hydrophilic block consisting of ethyleneoxy side chains.[21,26] In this study, we varied N and S independently as indicated in Table 1 (compounds **1**−**4**). The parameters a, b, and c in Table 1 are the dimensions of the unit cells determined by X-ray scattering. We borrow the crystal dimension nomenclature (a, b, c) used previously.[20,21,27]

Peptoids **1**−**4** were synthesized by the solid-phase submonomer method[28] and acetylated at their N termini.[29] The peptoids were purified by reverse phase high performance liquid chromatography (HPLC) using a cyano column to >90% molecular purity. The synthesis methods and analytical characterization are described in detail in the SI. Small-angle and wide-angle X-ray scattering (SAXS and WAXS) measurements were performed at ALS beamline 7.3.3[30] and at SSRL beamline 1−5. An atomistic model of bulk Ac-Ndc_9-Nte_9 was constructed using molecular dynamics (MD) simulations with the CHARMM-based[31] force field for peptoid backbones, MFTOID.[32]

The modeling of peptoids is necessary to interpret their X-ray scattering data in the context of a specific molecular conformation. To our knowledge, there is no extended *cis* backbone conformation model with which to interpret bulk phase peptoid polymer scattering in the literature. We therefore performed two MD simulations of periodic boxes consisting of 288 molecules of compound **1** (Ac-Ndc_9-Nte_9), one simulation starting from a *cis* and one starting from a *trans* backbone conformation. The *cis* backbone starting conformation was similar to that of the omega strand, which has been experimentally observed in constrained peptoid trimers,[33] and the *trans* backbone starting configuration was similar to that of the sigma strand, which is a computational model of a peptoid 28mer within a supramolecular nanosheet assembly.[34] Of the four peptoids we synthesized, we chose to model peptoid **1** because it had been previously reported to form crystalline assemblies.[26] The simulations were run for about 120 ns in an isothermal−isobaric (NPT) ensemble at 298 K and 1 atm pressure where all three orthogonal box dimensions were allowed to fluctuate independently (details in SI).

Typical molecular conformations obtained at the end of the simulation for the *cis* and *trans* backbone assemblies are shown in Figure 2. We show three views: one perpendicular to the backbone, one along the backbone, and one at a nonorthogonal angle to the backbone. We additionally show finer backbone structure with characteristic distances; the red arrows display the backbone width, and the black arrows display the length of two peptoid monomers along the backbone direction. It is evident that in both simulations, the relaxed molecules remain extended, and roughly planar. They appear to be confined to a board-like box as depicted in Figure 2. As expected, the *trans* conformation is more extended along the backbone direction than the *cis* conformation. The Nte block exhibits more disorder than the Ndc block. This is clearer in the case of the *trans* backbone; compare views along the backbone in Figure 2.

It is clear that the simulations starting from the *cis* and *trans* conformation initial conditions do not relax to the same equilibrium configuration. We posit that this is due to the infrequency of *cis*−*trans* isomerization in our simulation, which has slow kinetics compared to simulation time.[32,35] We estimated the absolute Gibbs free energies of the bulk phase of the Ac-Ndc_9-Nte_9 in *cis* and *trans* backbone conformations using the two-phase thermodynamics (2PT) method.[36−38] With this method, one can calculate equilibrium thermodynamic properties of condensed phases from relatively short MD trajectories without thermodynamic integration. The entropic contribution to the free energy is estimated by using the power spectrum, i.e., the vibrational density of states.[36] Our calculations (details in SI) show that the Gibbs free energy of the relaxed *cis* backbone conformation is lower than that of the *trans* backbone conformation: the difference is approximately 158 kJ/mol peptoid (8.8 kJ/mol per monomer), suggesting that the relaxed *cis* backbone conformation is closer to the global free energy minimum.

We used SAXS and WAXS to determine the unit cell dimensions for peptoids **1** through **4**. Figure 3A shows SAXS intensity versus magnitude of the scattering vector, q. For Ac-Ndc_9-Nte_9, we see two peaks q = 0.120 and q = 0.255 $Å^{-1}$, corresponding to spatial dimensions ($2\pi/q$) of 52.3 and 24.6 Å, respectively. These dimensions are very close to the b dimension of 51.9 Å and c dimension of 24.6 Å calculated from the *cis* backbone simulation, and less consistent with the b dimension of 57.4 Å and c dimension of 19.6 Å calculated from the *trans* backbone simulation. We therefore label these scattering peaks in Figure 3A as b (010) and c (001) in accordance to the *cis* backbone model. The values for N and S for Ac-Ndc_9-Nte_9 are 18 and 10. For each polymer in Figure 3A, N and S are labeled, and the c peak shifts to lower q with increasing S, whereas the b peak shifts to lower q with increasing N. These observations are consistent with the molecular model displayed in Figure 2. It appears from this data

DOI: 10.1021/jacs.7b11891
J. Am. Chem. Soc. 2018, 140, 827−833

Table 1. Compiled Peptoids, Their Chemistry, and Dimensions from X-ray Scattering Data

	Polymer Nomenclature	Side chain 1 (R_1)	Side chain 2, if diblock (R_2)	*N*	*S*	*a* (Å)	*b* (Å)	*c* (Å)	Author
1	Ac-Ndc_9-Nte_9			18	10	4.64	52.3	24.6	This work
2	Ac-Ndc_9-Nte_5			14	10	4.63	41.8	24.6	This work
3	Ac-Ndc_9-Nte_{15}			24	10	4.63	66.4	24.6	This work
4	Ac-Nhp_9-Nde_9			18	7	4.63	51.8	18.6	This work
5	Nia_6			6	4	- [a]	20.4	14.6	Rosales[19]
6	Nia_{15}			15	4	4.60	45.5	14.6	Rosales[19]
7	Nbu_{15}			15	4	4.53	44.4[b]	13.4	Rosales[19]
8	Nhx_{15}			15	6	4.56	-[c]	-[c]	Rosales[19]
9	Noc_{15}			15	8	4.56	50.6[b]	17.8	Rosales[19]
10	Npe_{15}			15	6	4.5	48.8	17.0	Rosales[19]
11	c-Nbu_{120}[d]			120	4	-[e]	-[d]	13	Lee[20]
12	c-Nhx_{72}[d]			72	6	-[e]	-[d]	16	Lee[20]
13	c-Noc_{88}[d]			88	8	4.6	-[d]	20	Lee[20]
14	c-Ndc_{133}[d]			133	10	4.5	-[d]	24	Lee[20]
15	c-$Nddc_{133}$[d]			133	12	4.5	-[d]	27	Lee[20]
16	c-$Nttdc_{30}$[d]			30	14	4.4	-[d]	33	Lee[20]
17	Ndc_9-Nte_{27}			36	10	4.5	104	25	Sun[21]
18	Ndc_{12}-Nte_{21}			33	10	4.5	99	25	Sun[21]
19	Ndc_{18}-Nte_{18}			36	10	4.5	108	25	Sun[21]
20	Ndc_{24}-Nte_{12}			36	10	4.5	113	25	Sun[21]
21	$NClPe_6$-Nce_6			12	7	4.5	33	18	Jin[23]
22	Nce_6-$NClPe_6$			12	7	4.5	35	18	Jin[23]

[a]The presence of many peaks in the vicinity occluded a precise *a* determination. [b]These values came from WAXS peaks very near the beamstop, limiting their accuracy; these points are not included in Figure 4 or linear regression fits. [c]These values were not included due to the reported concern about "an effect of the thermal history of the sample". [d]These samples were polymerized homogeneously in solution as a cyclic polymer; their *b* cannot be measured because of the polydispersity and cyclic nature. [e]The peak corresponding to *a* coincides with a peak corresponding to a higher order of *c*, and cannot be deconvoluted without additional fitting.

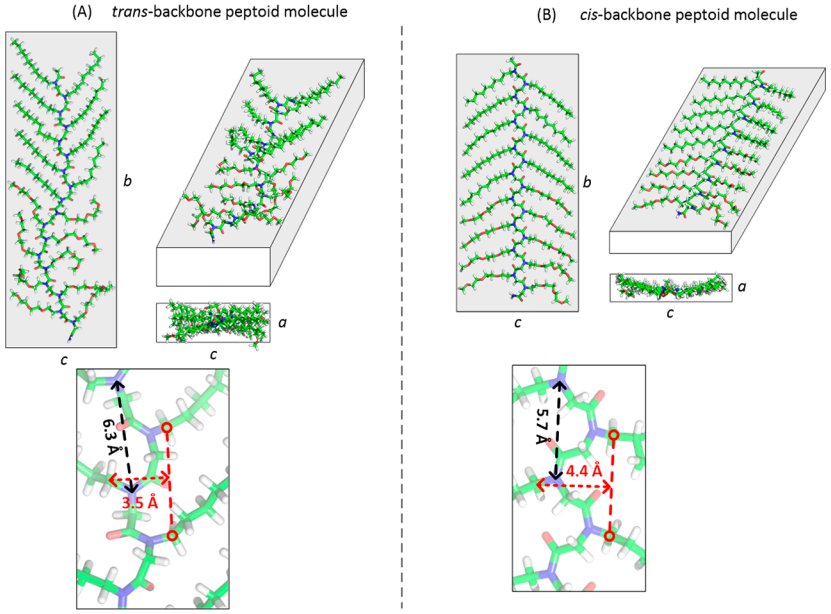

Figure 2. Relaxed molecular conformations *cis* and *trans* backbones are displayed. Each molecule is a representative taken from a 288-molecule MD simulation and is shown from three angles. The backbone in each conformation is displayed in higher detail, and the approximate width (red) and twice monomeric length (black) is given.

DOI: 10.1021/jacs.7b11891
J. Am. Chem. Soc. 2018, 140, 827−833

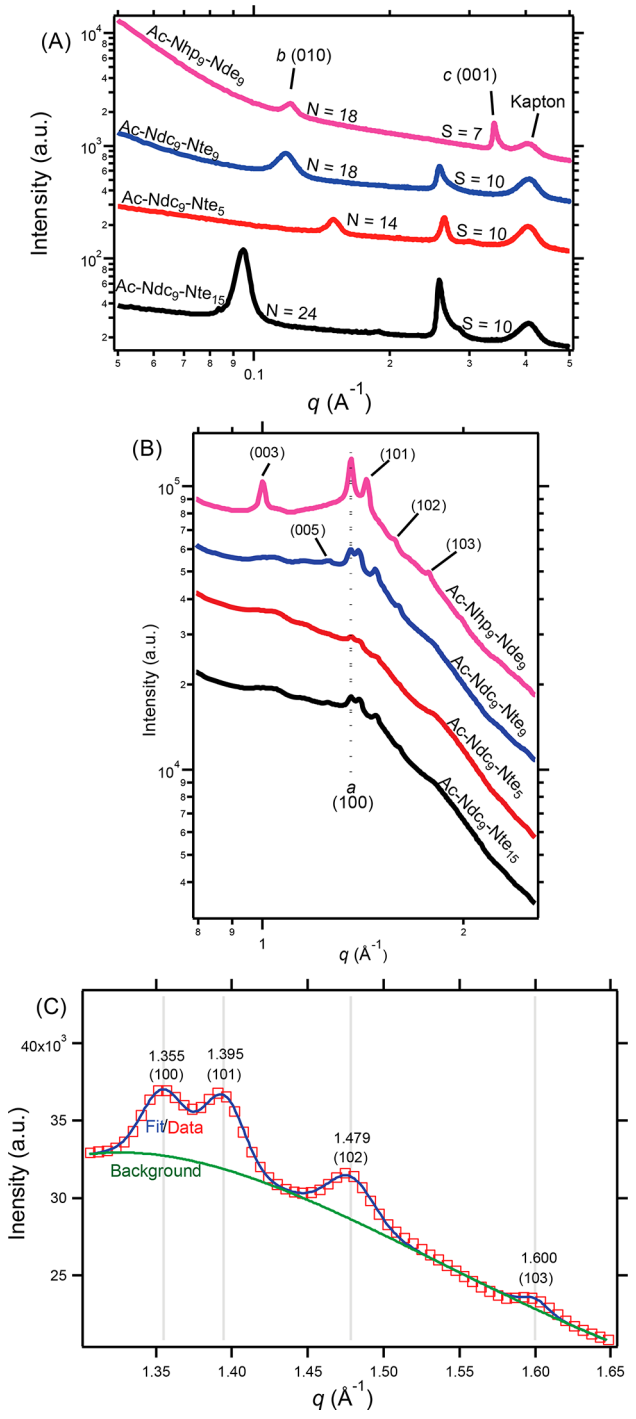

Figure 3. X-ray scattering measurements for compounds **1**–**4** (Table 1), plotted as intensity in arbitrary units vs scattering vector q. The traces are offset vertically for clarity. (A) In the small angle regime, the peaks corresponding to the b and c dimensions can be seen. (B) In the wide angle regime, the peaks corresponding to the a spacing can be seen, along with some higher order reflections. (C) The high-q data and fit for Ac-Ndc$_9$-Nte$_9$, with the peaks indexed and their q positions labeled. The fit is plotted in blue on top of the data, and the background fit is shown in green.

that the b dimension is independent of S, and the c dimension is independent of N. Figure 3B shows WAXS intensity versus magnitude of the scattering vector, q. For Ac-Ndc$_9$-Nte$_9$ (peptoid **1**), we see a peak at q = 1.35 Å^{-1}, corresponding to spatial dimensions of 4.63 Å. This dimension is very close to the a dimension of 4.6 Å obtained from the *cis* backbone simulation, as opposed to the a dimension of 4.7 Å obtained from the *trans* backbone simulation. We therefore label this scattering peak in Figure 3A as a (100). The WAXS profiles from peptoids **2**–**4** (Figure 3B) also contain a peak at the same q. It is evident that a is independent of both N and S, as suggested from the molecular model displayed in Figure 2B. The a, b, and c spacings for these four polymers are listed in Table 1, and were calculated by fitting Gaussian functions to the peaks.

We further identified the higher order peaks present in the WAXS data in Figure 3B, which inform the relationship between a and c. Figure 3C displays the higher order reflections for Ac-Ndc$_9$-Nte$_9$. The peaks found in this regime are due to reflections from the (100), (101), (102), and (103) planes, assuming an angle of 93.6° between a and c directions. A visualization of these crystal planes is provided in Figure S3. The curve in Figure 3C is a fit through the experimental data with the higher order peak locations at q values specified by using the a and c dimensions given in Table 1 and an angle of 93.6 degrees between these dimensions. In Figure 2, we have neglected the difference between 93.6° and 90°. The same fitting procedure was used to analyze the WAXS data from the other three peptoids in Figure 4B. The angles between a and c for the other Ndc-containing polymers (S = 10) were approximately 93.6 as well, and angle between a and c for Ac-Nhp$_9$-Nde$_9$ (S = 7) was 96.1°. We posit that these small deviations from orthogonality relieve intermolecular steric repulsions between side-chain $-CH_3$ groups adjacent in the c direction (Figure S3). Higher order reflections corresponding to the c direction, (003) and (005) are also seen in the WAXS data. With all the WAXS peaks accounted for, it is notable that no peaks were observed which could be assigned to other aspects of the crystalline structure such as side chain crystallinity. We posit that coherent scattering from the unit cell overwhelms other contributions. Taken together, this data indicate that the chains adopt a board-like planar shape with an all-*cis* backbone conformation, and are packed in lattices with main chains parallel to one another in the a and c dimensions.

In order to explore the generality of this molecular conformation and chain packing motif, we examined 18 additional crystalline polymers previously reported in the literature. We found four other studies that reported X-ray scattering from crystalline peptoid polymers (peptoids **5**–**22**, Table 1). In this set, there are 12 homopolymers with hydrocarbon side chains, and 10 diblock copolymers with a hydrophilic block and a crystalline hydrophobic block. Taken together, these polymers cover a wide range of backbone and side-chain lengths: N varies from 6 to 133, whereas S varies from 4 to 14. We pooled lattice dimensions taken from X-ray scattering data for all 22 compounds in Figure 4, wherein the relationship between the a, b, and c dimensions and N and S are examined. The relationships between molecular structure and crystal structure found in our study of peptoids **1**–**4** appear to be universal to all known peptoid polymer crystals.

We first explored the a dimension of all peptoid polymers plotted as a function of side chain length, S (Figure 4A). The a dimension is not dependent on S or N. The mean value of a is 4.55 ± 0.02 Å. The origin of the WAXS peaks in peptoid polymers is the subject of some controversy. Sun et al.[21] and Jin et al.[23] ascribed the (100) peak to the distance between adjacent backbones, consistent with the interpretation presented in this paper. However, Lee et al.[20] have ascribed

DOI: 10.1021/jacs.7b11891
J. Am. Chem. Soc. 2018, 140, 827–833

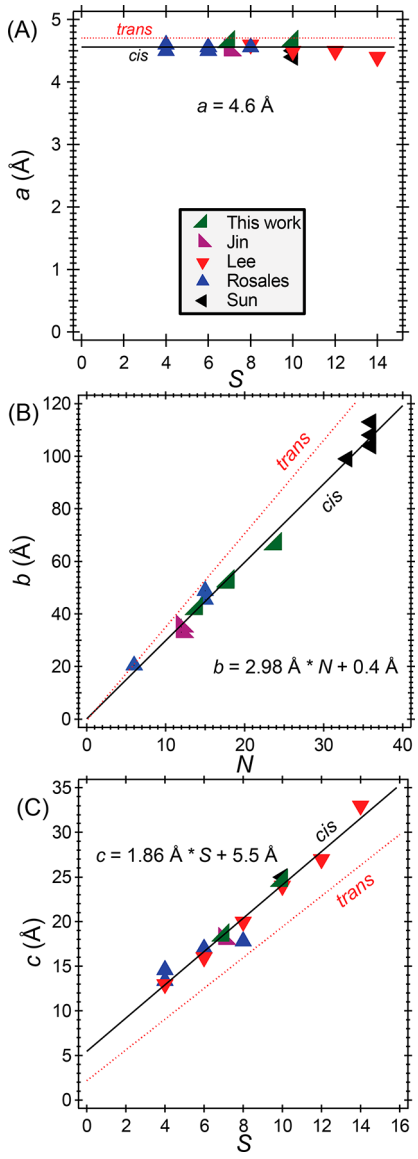

Figure 4. Collection of *a*, *b*, and *c* dimensions taken from the scattering data listed in Table 1. (A) The *a* dimension of peptoid polymers is always seen around 4.6 Å regardless of the side chain, arranged here by *S*. (B) The *b* spacing increases linearly with *N*. (C) The *c* spacing increases linearly with *S* and has an intercept of 5.5 Å. In all plots, the calculated trend for the *trans* conformation is displayed as a dashed red line for reference. The linear fits (solid black line) in all plots are consistent with the *cis* conformation but not the *trans* conformation.

this peak to side-chain crystallization without specifying a particular plane, whereas Rosales et al.[19] assume a hexagonal crystal and assign the WAXS peak corresponding to the spatial dimension of about 4.6 Å to reflections from the (300) planes. Neither Lee et al.[20] nor Rosales et al.[19] were able to explain the presence of all the observed WAXS peaks. To our knowledge, the unit cell proposed in this study is the only interpretation that is consistent with all the observed WAXS peaks for all *S* and *N* (see Figure 3B,C). Therefore, when compiling data for Table 1, the lowest *q* peak in the WAXS regime that cannot be attributed to higher order reflections of *b* and *c* dimensions gives the *a* dimension. We used our simulations of peptoid **1** (Figure 2) to calculate the expected *a* dimension for *cis* and *trans* backbone conformations. This calculation was performed by measuring distances between nitrogen atoms on molecules adjacent in the *a* direction. These *a* dimensions are 4.6 Å for the *cis* backbone and 4.7 Å for the *trans* backbone, which are close but readily distinguishable. In an important study, Mannige et al.[34] performed MD simulations and calculated an *a* dimension of 4.7 Å in *trans* backbone peptoids. The *a* dimension of the polymers in Table 1 is more consistent with *cis* backbone models than *trans* backbone models.

We next examined the *b* dimension of the peptoids polymers as a function of main chain length, *N* (Figure 4B). It is evident from the scattering data that *b* is a linear function of *N*. The linear fit through these data gives b (Å) = $[2.98 \pm 0.08]N + [0.35 \pm 1.70]$, $r^2 = 0.99$. The *b* dimension is proportional to backbone length and independent of side-chain length. One can also calculate the relationship between *b* and *N* using a molecular model. In our *cis* simulation, we found the distance between adjacent monomers on the same side of the backbone to be 5.7 Å (see Figure 2B), which corresponds to *b* being a linear function of 2.9 Å per monomer. In contrast, Mannige et al.[34] reported this value to be 3.5 Å per monomer in an all-*trans* model of an extended peptoid. The dotted line in Figure 4B shows the expected *b* versus *N* relationship if this were true. The measured slope of 2.98 Å per monomer in Figure 4B is consistent with the peptoid *cis* conformation, and not in the *trans* conformation. The value of the linear fit at $N = 18$ is 54.0 Å, which is consistent with the dimension of 51.9 Å calculated from our *cis* backbone simulation and not consistent with the dimension of 57.4 Å calculated from our *trans* backbone simulation.

Finally, we examined the *c* dimension of the peptoid polymers as a function of the side-chain length, *S* (Figure 4C). The side-chain length, *S*, is defined as the number of non-hydrogen atoms contained in an equivalent linear side chain. In side chains that are branched, we exclude the redundant branches, and in side chains containing a phenyl group, the redundant *ortho* and *meta* carbon are not counted. The *c* spacing increases linearly with side-chain length and the fit gives c (Å) = $[1.86 \pm 0.10]S + [5.5 \pm 0.8]$, $r^2 = 0.97$. It is evident that *c* is independent of *N*. Note that the intercept of the fit is 5.5 Å. This length represents the *c* dimension of a hypothetical peptoid crystal as the side-chain length approaches zero. One can readily estimate the expected intercept from a molecular model. As shown in Figure 2, these intercepts are 4.4 Å for *cis* and 3.5 Å for *trans* backbones. For both cases, these values are calculated by projecting the polymer into the plane normal to *a* and calculating the distance between an α carbon side-chain atom and the line connecting the two α carbon side-chain atoms on the opposite side of the backbone (see red arrows in Figure 2). The simulations also enable determination of the *c* dimension for $S = 10$ (box size in Figure 2): $c = 24.6$ Å for the *cis* backbones and $c = 19.6$ Å for the *trans* backbones. Assuming a linear relationship between *c* and *S*, the simulations predict the slope of this relationship to 2.02 Å for *cis* and 1.61 Å for *trans*. The dotted line in Figure 4C shows the expected relationship for *trans* backbones. The measured slopes and intercepts, 1.86 and 5.5 Å, are much closer to those obtained from the *cis* simulations.

The peptoid diblock copolymers **1**−**4** and **17**−**22** all self-assemble to form crystalline nanosheets in water. We used WAXS to examine the nanosheet form of compound **1** and compared it to its structure in the bulk phase to reveal the structural similarities (Figure 5). WAXS traces were obtained from a 6 mg/mL aqueous solution of Ac-Ndc_9-Nte_9 as well as

DOI: 10.1021/jacs.7b11891
J. Am. Chem. Soc. 2018, 140, 827−833

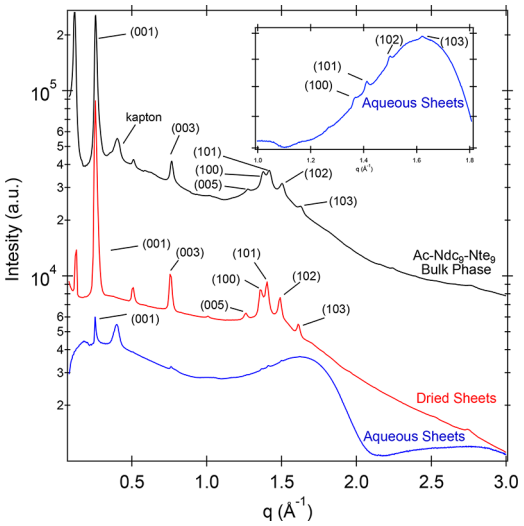

Figure 5. WAXS scattering of Ac-Ndc$_9$-Nte$_9$ in bulk, as aqueous nanosheets with a subtraction for water, and as dried nanosheets. Traces are offset vertically for clarity and peaks are labeled. Inset is of aqueous sheets at high q. Peak locations and indexing are consistent among samples.

from dried nanosheets and from a bulk sample. The peak locations in all three samples are identical. Therefore, our conclusion regarding the prevalence of the extended, all-*cis* conformation applies to both bulk crystals and aqueous diblock nanosheets. In addition, the dependence of a, b, and c on S and N given above also applies to these diblock nanosheets.

CONCLUSION

We present a universal relationship between the molecular structure and crystal structure of peptoid homopolymers and diblock copolymers. Our conclusions are based on X-ray scattering and molecular dynamics simulations. The crystal dimensions are simple linear functions of main-chain length N and side-chain length S:

$$a\ (\text{Å}) = 4.55 \pm 0.02$$

$$b\ (\text{Å}) = [2.98 \pm 0.08]N + [0.35 \pm 1.70]$$

$$c\ (\text{Å}) = [1.86 \pm 0.10]S + [5.5 \pm 0.8]$$

These relationships, which apply to all 22 known crystalline peptoid polymers, indicate the prevalence of the *cis* backbone conformation, despite numerous previous studies which either implicitly or explicitly assumed a *trans* peptoid backbone.[19−23,25,27,34,39] These relationships reveal a common, extended backbone conformation that display the side chains in an apposed geometry, creating a planar, board-like shape. Furthermore, in both the bulk phase and in aqueous nanosheets, these polymers pack together with their backbones in close contact and alignment with one another. This suggests that the all-*cis* peptoid backbone itself is capable of forming multiple weak interchain attractive interactions, likely the result of CH−O hydrogen bonding[40,41] or amide dipole interactions.[42] This new structural motif can be used to design broad classes of assemblies which have specific unit cell sizes, functional group densities, or nanosheet thicknesses, based upon a specific backbone conformation and packing preference.

ASSOCIATED CONTENT

Supporting Information

The Supporting Information is available free of charge on the ACS Publications website at DOI: 10.1021/jacs.7b11891.

Peptoid synthesis, nanosheet formation, X-ray scattering methods, molecular dynamic simulation, atomic coordinate file for peptoid model, schematic indicating crystal planes, and peptoid characterization and purity (PDF)
Structure model (PDB)

AUTHOR INFORMATION

Corresponding Authors

*nbalsara@berkeley.edu
*rnzuckermann@lbl.gov

ORCID

Ryan K. Spencer: 0000-0002-1043-3913
Tod Pascal: 0000-0003-2096-1143
Ronald N. Zuckermann: 0000-0002-3055-8860

Present Address

⊥Department of Chemistry, Duke University, Durham, North Carolina 27708 United States

Notes

The authors declare no competing financial interest.

ACKNOWLEDGMENTS

The work was funded primarily by the Soft Matter Electron Microscopy Program (KC11BN), supported by the Office of Science, Office of Basic Energy Science, US Department of Energy, under Contract DE-AC02-05CH11231. Work at the Molecular Foundry, the Advanced Light Source and the High Performance Computing Services Group at Lawrence Berkeley National Laboratory was supported by the Office of Science, Office of Basic Energy Science, US Department of Energy, under Contract DE-AC02-05CH11231. Use of the Stanford Synchrotron Radiation Lightsource, SLAC National Accelerator Laboratory, is supported by the U.S. Department of Energy, Office of Science, Office of Basic Energy Sciences under Contract No. DE-AC02-76SF00515. We gratefully acknowledge Dr. John R. Edison and Dr. Stephen Whitelam for their discussions on molecular model building.

REFERENCES

(1) Simon, R. J.; Kania, R. S.; Zuckermann, R. N.; Huebner, V. D.; Jewell, D. A.; Banville, S.; Ng, S.; Wang, L.; Rosenberg, S.; Marlowe, C. K. *Proc. Natl. Acad. Sci. U. S. A.* **1992**, *89*, 9367.
(2) Gangloff, N.; Ulbricht, J.; Lorson, T.; Schlaad, H.; Luxenhofer, R. *Chem. Rev.* **2016**, *116*, 1753.
(3) Zhang, D.; Lahasky, S. H.; Guo, L.; Lee, C.-U.; Lavan, M. *Macromolecules* **2012**, *45*, 5833.
(4) Sun, J.; Zuckermann, R. N. *ACS Nano* **2013**, *7*, 4715−4732.
(5) Fowler, S. A.; Blackwell, H. E. *Org. Biomol. Chem.* **2009**, *7*, 1508.
(6) Rosales, A. M.; Segalman, R. A.; Zuckermann, R. N. *Soft Matter* **2013**, *9*, 8400.
(7) Knight, A. S.; Zhou, E. Y.; Francis, M. B.; Zuckermann, R. N. *Adv. Mater.* **2015**, *27*, 5665.
(8) Robertson, E. J.; Battigelli, A.; Proulx, C.; Mannige, R. V.; Haxton, T. K.; Yun, L.; Whitelam, S.; Zuckermann, R. N. *Acc. Chem. Res.* **2016**, *49*, 379.
(9) Rosales, A. M.; Murnen, H. K.; Kline, S. R.; Zuckermann, R. N.; Segalman, R. A. *Soft Matter* **2012**, *8*, 3673.
(10) Gao, Y.; Kodadek, T. *Chem. Biol.* **2013**, *20*, 360.
(11) Crapster, J. A.; Guzei, I. A.; Blackwell, H. E. *Angew. Chem., Int. Ed.* **2013**, *52*, 5079.

DOI: 10.1021/jacs.7b11891
J. Am. Chem. Soc. 2018, 140, 827−833

(12) Huang, K.; Wu, C. W.; Sanborn, T. J.; Patch, J. A.; Kirshenbaum, K.; Zuckermann, R. N.; Barron, A. E.; Radhakrishnan, I. *J. Am. Chem. Soc.* **2006**, *128*, 1733.
(13) Gorske, B. C.; Mumford, E. M.; Gerrity, C. G.; Ko, I. *J. Am. Chem. Soc.* **2017**, *139*, 8070.
(14) Wu, C. W.; Sanborn, T. J.; Huang, K.; Zuckermann, R. N.; Barron, A. E. *J. Am. Chem. Soc.* **2001**, *123*, 6778.
(15) Tedesco, C.; Erra, L.; Izzo, I.; De Riccardis, F. *CrystEngComm* **2014**, *16*, 3667.
(16) Shin, S. B. Y.; Yoo, B.; Todaro, L. J.; Kirshenbaum, K. *J. Am. Chem. Soc.* **2007**, *129*, 3218.
(17) Zuckermann, R. N.; Kerr, J. M.; Moos, W. H.; Kent, S. B. H. *J. Am. Chem. Soc.* **1992**, *114*, 10646.
(18) Lutz, J.-F.; Ouchi, M.; Liu, D. R.; Sawamoto, M. *Science (Washington, DC, U. S.)* **2013**, *341*, 1238149.
(19) Rosales, A. M.; Murnen, H. K.; Zuckermann, R. N.; Segalman, R. A. *Macromolecules* **2010**, *43*, 5627.
(20) Lee, C. U.; Li, A.; Ghale, K.; Zhang, D. *Macromolecules* **2013**, *46*, 8213.
(21) Sun, J.; Teran, A. A.; Liao, X.; Balsara, N. P.; Zuckermann, R. N. *J. Am. Chem. Soc.* **2014**, *136*, 2070.
(22) Sun, J.; Jiang, X.; Lund, R.; Downing, K. H.; Balsara, N. P.; Zuckermann, R. N. *Proc. Natl. Acad. Sci. U. S. A.* **2016**, *113*, 3954.
(23) Jin, H.; Jiao, F.; Daily, M. D.; Chen, Y.; Yan, F.; Ding, Y.-H.; Zhang, X.; Robertson, E. J.; Baer, M. D.; Chen, C.-L. *Nat. Commun.* **2016**, *7*, 12252.
(24) Jiao, F.; Chen, Y.; Jin, H.; He, P.; Chen, C. L.; De Yoreo, J. J. *Adv. Funct. Mater.* **2016**, *26*, 8960.
(25) Murnen, H. K.; Rosales, A. M.; Jaworski, J. N.; Segalman, R. A.; Zuckermann, R. N. *J. Am. Chem. Soc.* **2010**, *132*, 16112.
(26) Sun, J.; Jiang, X.; Lund, R.; Downing, K. H.; Balsara, N. P.; Zuckermann, R. N. *Proc. Natl. Acad. Sci. U. S. A.* **2016**, *113*, 3954.
(27) Kortright, J. B.; Sun, J.; Spencer, R. K.; Jiang, X.; Zuckermann, R. N. *J. Phys. Chem. B* **2017**, *121*, 298.
(28) Tran, H.; Gael, S. L.; Connolly, M. D.; Zuckermann, R. N. *J. Visualized Exp.* **2011**, *57*, No. e3373.
(29) Kim, S.; Biswas, G.; Park, S.; Kim, A.; Park, H.; Park, E.; Kim, J.; Kwon, Y.-U. *Org. Biomol. Chem.* **2014**, *12*, 5222.
(30) Hexemer, A.; Bras, W.; Glossinger, J.; Schaible, E.; Gann, E.; Kirian, R.; MacDowell, A.; Church, M.; Rude, B.; Padmore, H. *J. Phys. Conf. Ser.* **2010**, *247*, 012007.
(31) Brooks, B. R.; Brooks, C. L.; Mackerell, A. D.; Nilsson, L.; Petrella, R. J.; Roux, B.; Won, Y.; Archontis, G.; Bartels, C.; Boresch, S.; Caflisch, A.; Caves, L.; Cui, Q.; Dinner, A. R.; Feig, M.; Fischer, S.; Gao, J.; Hodoscek, M.; Im, W.; Kuczera, K.; Lazaridis, T.; Ma, J.; Ovchinnikov, V.; Paci, E.; Pastor, R. W.; Post, C. B.; Pu, J. Z.; Schaefer, M.; Tidor, B.; Venable, R. M.; Woodcock, H. L.; Wu, X.; Yang, W.; York, D. M.; Karplus, M. *J. Comput. Chem.* **2009**, *30*, 1545.
(32) Mirijanian, D. T.; Mannige, R. V.; Zuckermann, R. N.; Whitelam, S. *J. Comput. Chem.* **2014**, *35*, 360.
(33) Gorske, B. C.; Mumford, E. M.; Conry, R. R. *Org. Lett.* **2016**, *18*, 2780.
(34) Mannige, R. V.; Haxton, T. K.; Proulx, C.; Robertson, E. J.; Battigelli, a; Butterfoss, G. L.; Zuckermann, R. N.; Whitelam, S. *Nature* **2015**, *526*, 415.
(35) Sui, Q.; Borchardt, D.; Rabenstein, D. L. *J. Am. Chem. Soc.* **2007**, *129*, 12042.
(36) Lin, S.-T.; Blanco, M.; Goddard, W. A. *J. Chem. Phys.* **2003**, *119*, 11792.
(37) Lin, S.-T.; Maiti, P. K.; Goddard, W. A. *J. Phys. Chem. B* **2010**, *114*, 8191.
(38) Pascal, T. A.; Lin, S.-T.; Goddard, W. A., III *Phys. Chem. Chem. Phys.* **2011**, *13*, 169.
(39) Murnen, H. K.; Rosales, A. M.; Dobrynin, A. V.; Zuckermann, R. N.; Segalman, R. A. *Soft Matter* **2013**, *9*, 90.
(40) Baures, P. W.; Beatty, A. M.; Dhanasekaran, M.; Helfrich, B. A.; Pérez-Segarra, W.; Desper, J. *J. Am. Chem. Soc.* **2002**, *124*, 11315.
(41) Angelici, G.; Bhattacharjee, N.; Roy, O.; Faure, S.; Didierjean, C.; Jouffret, L.; Jolibois, F.; Perrin, L.; Taillefumier, C. *Chem. Commun.* **2016**, *52*, 4573.
(42) Paulini, R.; Müller, K.; Diederich, F. *Angew. Chem., Int. Ed.* **2005**, *44*, 1788.

DOI: 10.1021/jacs.7b11891
J. Am. Chem. Soc. 2018, 140, 827−833